

Optimization of Kumada-Corriu-Tamao cross-coupling reactions of tri- and tetra- bromothiophenes and symmetrical di-bromo-2, 2' bithiophene with cyclohexylmagnesium bromide: Synthesis, DFT studies and nonlinear optical analysis

Adnan A. Dahadha ^{1*}, Mohammad Abunuwar ² Mohammad Al-Dhoun ²,
Mohammed Hassan ³ and Mohamed J. Saadh ⁴

¹Department of Biotechnology and Genetic Engineering, Faculty of Science, Philadelphia University, Amman, Jordan

²Faculty of Pharmacy, Philadelphia University, Amman, Jordan.

³Department of Chemistry, Faculty of Science, Ibb University, Ibb, Yemen.

⁴Faculty of Pharmacy, Middle East University, Amman, Jordan

(Received June 07, 2022; Revised July 30, 2022; Accepted August 14, 2022)

Abstract: Tri-, tetra-bromothiophene and symmetrical dibromo-2,2'-bithiophene derivatives were coupled efficiently with cyclohexylmagnesium bromide in the presence of iron, nickel and palladium as catalysts under optimized mild reaction conditions. Additives such as lithium chloride and bromide were employed to enhance the efficiency of the Grignard reagent. The corresponding coupled products, which were widely used as precursors or additives in photonic industries were studied by DFT method at B3LYP/6-311++G(d,p) level of theory using Gaussian 09W to explore the global chemical reactivity descriptors and nonlinear optical activities (NLO). According to the results of NLO analysis, polarizability (α), anisotropy hyperpolarizability ($\Delta\alpha$) and first order hyperpolarizability (β) exhibited higher value than the standard urea, which reflect a promising molecular non-linear susceptibility, indicating that the compounds **4a-4f** are good candidates in the potential photonic applications.

Keywords: Iron; nickel; palladium; thiophene; nonlinear optical analysis. ©2022 ACG Publication. All right reserved.

1. Introduction

Cross-coupling reactions are straightforward and versatile method in organic synthesis for the formation of substantial building blocks of many naturally occurring molecules, polymers and biologically active compounds.^{1, 2} The advances in the transition metal catalysis have enhanced the coupling of organic electrophiles with organometallic nucleophiles with high efficiencies and broad substrate scopes, such as preparation of significant alkylated and arylated heteroaromatic compounds.³⁻⁵ The Kumada-Corriu-Tamao coupling, in which an organic electrophilic substrate is coupled to a Grignard nucleophile was explored at the very early stage of modern cross-coupling chemistry.⁶ In comparison with the other cross-coupling protocols, Grignard reagents remain acceptable coupling partners in Kumada-Corriu-Tamao coupling due to their low cost, easy to prepare and commercial availability.⁷ Furthermore, many other organometallic coupling partners are made from the corresponding Grignard reagents as starting materials in Negishi coupling.⁸ While, Suzuki cross-coupling required to the corresponding boronic acid esters, which would be purchased or synthesized, moreover, stoichiometric amount of a base has to be applied to generate quite

* Corresponding author: E-Mail: adnan.dahadha_chem@yahoo.com

Optimization of Kumada cross-coupling reactions

substantial amount of waste.⁹ Thus, the Kumada-Corriu-Tamao coupling gives straightforward access to the same desired coupled products without consuming additional reaction steps.

Organic compounds with heteroaromatic parts have received increasing attention as promising precursors of electrical and optical materials. In general, oligothiophenes have electroluminescent behaviours and an excellent conductivity.^{10,11} Conducting conjugated polymers such as polypyrrole and polythiophene are generally insoluble and infusible materials because of their high molecular weights.^{12,13} Various cyclohexyl end-capped oligomeric semiconductors based on oligothiophenes have been prepared *via* Stille and Suzuki cross-couplings, where the cyclohexyl group provides the oligomers with steric bulkiness at the periphery of the molecules for enhanced solubility without having a detrimental influence on the molecular packing in the thin film phase.¹⁴ In the same context, polythiophenes, such as poly(3-cyclohexylthiophenes), attracted considerable attention for their optical properties, stability and electrical conductivity.¹⁵ In turn, to achieve some sp^3 - sp^2 coupling reactions, applying Kumada-Corriu-Tamao coupling reaction, particular reagents like TMEDA (*N,N,N',N'*-tetramethylethylenediamine) as an additive and catalysts having pincer ligands are required.^{16,17} Nevertheless, the optimized protocol for alkyl-alkyl Kumada-Corriu-Tamao coupling has been inefficient for alkyl-aryl or alkyl- heterocyclic coupling, hence, amine ligands and additives such as TMEDA were widely employed to promote alkyl-aryl Kumada-Corriu-Tamao coupling.^{18,19}

Herein, an efficient synthetic protocol for cross coupling of cyclohexyl magnesium bromide (C_{SP}^3 nucleophile) with various tri- and tetrabromothiophene and symmetrical dibromo-2, 2'-bithiophene derivatives (C_{SP}^2 electrophile) under normal conditions using common palladium, nickel and iron complexes of general formula $[MCl_2(dppx)]$ ($x = (CH_2)_n$, $n = 1, 2, 3$; dpp = diphenylphosphino alkane) and lithium halide adducts of Grignard reagents, which showed an enhanced reactivity, is reported. In addition to enhancement of the catalytic activity of nickel and iron complexes, they were compared with catalytically active palladium complexes, which are typically utilized in cross-coupling reactions. Recently, the cross-coupling reactions catalyzed by iron complexes are one of the promising research areas for the construction of C-C bonds as they are cheap and environmentally friendly compared to palladium and nickel. However, currently optimized synthetic protocol in the presence of iron, nickel and palladium has the advantage of low cost, ease and atom-economy in the preparation, and high reactivity with short reaction time. The resulting coupled products are good candidates as precursors in liquid crystalline materials, conducting polymers and solar cells.

Generally, molecules with nonlinear optical response to electromagnetic field have been extensively studied.²⁰⁻²² These molecules have numerous applications in photonics and optoelectronic devices such as light emitting diodes (LED) displays, optical storage, solar cells, optical fiber, and phototransistors.²³⁻²⁶ NLO susceptibility responses to electromagnetic field could be evaluated by theoretical modelling methods.^{27,28} In this work thiophene derivatives were applied to DFT calculation to determine their chemical reactivity and NLO properties.

2. Experimental

2.1. Chemical Material and Apparatus

Tri- and tetrabromothiophene and symmetrical dibromo-2,2'-bithiophene derivatives were purchased from Sigma Aldrich. Grignard reagents and the corresponding LiCl, LiBr and LiI adducts as well as the precatalysts $[FeCl_2(dppm)]$ **3a**, $[FeCl_2(dppe)]$ **3b**, $[FeCl_2(dppp)]$ **3c**, $[NiCl_2(dppm)]$ **3d**, $[NiCl_2(dppe)]$ **3e**, $[NiCl_2(dppp)]$ **3f**, $[PdCl_2(dppm)]$ **3g**, $[PdCl_2(dppe)]$ **3h**, and $[PdCl_2(dppp)]$ **3i**-were prepared following the literature procedures.²⁹⁻³¹ All starting materials were purchased from Sigma Aldrich and used without further purification. Molarity of the Grignard solutions were determined by the titration.³² All the reactions requiring catalyst were conducted under nitrogen atmosphere in freshly distilled anhydrous solvents.³³ Yields of the coupled products were determined by GC. NMR spectra were recorded on a Bruker AC 200 spectrometer (1H: 200 MHz, 13C: 50.32 MHz, $CDCl_3$ internal standard) as shown in figures S1-S12. Mass spectra were recorded on high resolution mass spectrometer Bruker Apex IV. 7 T (LC-MS).

2.2. General Procedure for Cross-Coupling Reactions.

In a typical experiment, a dry and nitrogen-flushed 50-mL Schlenk tube, equipped with a magnetic stirring bar, was charged with the respective tri- and tetra-bromothiophene and symmetrical dibromo-2,2'-bithiophene derivatives (160.0 mg for tribromothiophene and 200.0 mg for tetrabromothiophene derivatives), as well as 162.0 mg for symmetrical dibromo-2,2'-bithiophene derivatives, 3 mol% of the required catalyst was loaded in 15.0 ml of THF ([FeCl₂(dppm)]: 7.6 mg, [FeCl₂(dppe)]: 7.9 mg, [FeCl₂(dppp)]: 8.1 mg, [NiCl₂(dppm)]: 7.7 mg, [NiCl₂(dppe)]: 7.9 mg, [NiCl₂(dppp)]: 8.1 mg, [PdCl₂(dppm)]: 8.4 mg, [PdCl₂(dppe)]: 8.6 mg, [PdCl₂(dppp)]: 8.8 mg). The mixture was stirred for 5 min, then, cyclohexylmagnesium bromide or the LiCl or LiBr adduct (0.8 mmol, 4.0 ml of a 0.2M Grignard reagent) was rapidly added and the mixture was left stirring vigorously at room temperature for one hour. After the reaction mixture was hydrolyzed with diluted hydrochloric acid, the mixture was extracted with diethyl ether, washed with saturated NaCl solution and water. The organic layer was dried over MgSO₄, filtered and the solvent was evaporated under reduced pressure. The crude product was purified by column chromatography using hexane as an eluting solvent to obtain the corresponding pure product.

2, 3, 4-Tricyclohexyl Thiophene 4a: MS (EI)[(m/z, %)] : 330 (95) [M⁺], 247 (30) [M – Cyclohexyl]⁺, 165 (30) [M – 2 Cyclohexyl]⁺, 287 (80) [M – CH₂CH₂CH₃]⁺, 273 (50) [M – CH₂CH₂CH₂CH₃]⁺, ¹H NMR (CDCl₃, 200.13 MHz, 298 K) [ppm]: δ = 0.86 – 1.76 (m, 31H, CH₂), 2.16 – 2.49 (m, 3H, CH), 6.79 (Thiophene H1, S). ¹³C NMR (CDCl₃, 50.32 MHz) [ppm] : δ = 25.66(3CH), 26.73 (6CH₂), 26.93 (6CH₂), 27.46 (CH), 32.96 (CH), 37.98 (CH), 115.94 (C_{thio}H), 119.72 (C_{thio}), 134.35 (C_{thio}), 137.99 (C_{thio}).

2,3,5-Tricyclohexyl Thiophene 4b: MS (EI)[(m/z, %)] : 330 (60) [M⁺], 247 (100) [M – Cyclohexyl]⁺, 165 (80) [M – 2 Cyclohexyl]⁺, 287 (10) [M – CH₂CH₂CH₃]⁺, 273 (10) [M – CH₂CH₂CH₂CH₃]⁺, ¹H NMR (CDCl₃, 200.13 MHz, 298 K) [ppm]: δ = 0.86 – 1.73 (m, 31H, CH₂), 2.16 – 2.38 (m, 3H, CH), 6.97 (Thiophene H1, S). ¹³C NMR (CDCl₃, 50.32 MHz) [ppm] : δ = 26.99 (3CH), 27.31 (6CH₂), 27.55 (6CH₂), 28.03 (CH), 33.55 (CH), 38.68 (CH), 117.01 (C_{thio}H), 119.98 (C_{thio}), 136.06 (C_{thio}), 140.41 (C_{thio}).

2,3,4,5-Tetracyclohexyl Thiophene 4c: MS (EI)[(m/z, %)] : 412 (60) [M⁺], 329 (100) [M – Cyclohexyl]⁺, 246 (70) [M – 2 Cyclohexyl]⁺, ¹H NMR (CDCl₃, 200.13 MHz, 298 K) [ppm]: δ = 0.85 – 1.39 (m, 40H, CH₂), 1.43 – 1.95 (m, 4H, CH), ¹³C NMR (CDCl₃, 50.32 MHz) [ppm] : δ = 26.41 (4CH), 26.90 (8CH₂), 28.47 (8CH₂), 33.79 (2CH), 39.78 (2CH), 123.88 (2C_{thio}), 137.64 (2C_{thio}).

3,3-Dicyclohexyl-2,2'-bithiophene 4d: MS (EI)[(m/z, %)] : 330 (100) [M⁺], 247 (90) [M – Cyclohexyl]⁺, 164 (85) [M – 2 Cyclohexyl]⁺, 287 (35) [M – CH₃CH₂CH₂]⁺, ¹H NMR (CDCl₃, 200.13 MHz, 298 K) [ppm]: δ = 0.83 – 1.84 (m, 20H, CH₂), 2.15-2.30 (m, 2H, CH), 7.09 (Thiophene H1 and 1', dd, ³J= 4 Hz), 7.29 (Thiophene H2 and 2', dd, ⁴J= 4 Hz). ¹³C NMR (CDCl₃, 50.32 MHz) [ppm] : δ = 26.39 (2CH), 27.21 (4CH₂), 35.19 (4CH₂), 39.02 (2CH), 124.00 (2C_{thio}H), 127.68 (2C_{thio}H), 134.65 (2C_{thio}), 139.23 (2C_{thio}).

4,4-Dicyclohexyl-2,2'-bithiophene 4e: MS (EI)[(m/z, %)] : 330 (100) [M⁺], 247 (45) [M – Cyclohexyl]⁺, 164 (55) [M – 2 Cyclohexyl]⁺, 287 (10) [M – CH₃CH₂CH₂]⁺, ¹H NMR (CDCl₃, 200.13 MHz, 298 K) [ppm]: δ = 1.24 – 1.53 (m, 20H, CH₂), 1.72-1.89 (m, 2H, CH), 6.68 (Thiophene H1 and 1', dd, ⁴J= 2 Hz), 6.88 (Thiophene H2 and 2', dd, ⁴J= 2 Hz). ¹³C NMR (CDCl₃, 50.32 MHz) [ppm] : δ = 26.22 (2CH), 26.45 (4CH₂), 35.46 (4CH₂), 39.09 (2CH), 123.26 (2C_{thio}H), 127.00 (2C_{thio}H), 134.56 (2C_{thio}), 138.04 (2C_{thio}).

5,5-Dicyclohexyl-2,2'-bithiophene 4f: MS (EI)[(m/z, %)] : 330 (50) [M⁺], 247 (100) [M – Cyclohexyl]⁺, 164 (69) [M – 2 Cyclohexyl]⁺, 287 (20) [M – CH₃CH₂CH₂]⁺. ¹H NMR (CDCl₃, 200.13 MHz, 298 K) [ppm]: δ = 1.23 – 1.76 (m, 20H, CH₂), 2.34-2.49 (m, 2H, CH), 6.80 (Thiophene H1 and 1', dd, ³J= 4 Hz), 6.91 (Thiophene H2 and 2', dd, ³J= 4 Hz). ¹³C NMR (CDCl₃, 50.32 MHz) [ppm] : δ = 25.59 (2CH), 26.01 (4CH₂), 34.99 (4CH₂), 39.01 (2CH), 123.00 (2C_{thio}H), 126.71 (2C_{thio}H), 134.11 (2C_{thio}), 137.21 (2C_{thio}).

Optimization of Kumada cross-coupling reactions

2.3. DFT Method and Calculation

DFT studies were performed using Gaussian 09W software package²⁰, while visualization of the results and the plots of molecules were obtained by Gaussview 6.0 program. All calculations were achieved *via* B3LYP/6-311++G(d,p) basis set, which is considered as an accurate level of theory by allowing the atomic orbitals to be polarized. Hence, p-functions were added to the hydrogen atoms, whilst d-functions were added to the heavy atoms (non-hydrogen atoms).²¹⁻²⁴ In addition, a set of the diffuse functions were added to hydrogens and heavy atoms.

2.3.1. Global Reactivity Descriptors (GRDs)

The global reactivity descriptors, hardness (η), electronegativity (χ), chemical potential (μ), electron affinity (EA), ionization potential, electrophilicity index (ω), maximum charge transfer (ΔN_{\max}) and HOMO, LUMO energies, as well as energy gap (ΔE) were evaluated at the same level of theory using two phases: gas and solution (chloroform and acetone). The calculations were achieved *via* running energy job type on Gaussian 09W software. The unsubstituted thiophene ring was investigated by the calculations to explore the influence of addition of the cyclohexyl group to the thiophene ring. The similar calculations were also applied to Urea to reveal the effect of GRDs on Non-linear optical (NLO) properties; urea is often used as a standard in NLO analysis. Urea is an important molecule as it contains classical organic atoms and both single and double bonds; an accurate evaluation of its nonlinearities can then be useful for formulation of other interesting classes of organic nonlinear optical materials.²⁵ The unsubstituted thiophene and urea were evaluated at the same level of theory to achieve a reliable comparison of the various chemical reactivities for the coupled products **4a-4f**. The global reactivity parameters were evaluated by using the following equations (Table 1).

Table 1. Global reactivity descriptors

Global reactivity descriptor	Equation	Reference
Ionization potential (IP)	$IP = -E_{\text{HOMO}}$	[21]
Electron affinity (EA)	$EA = -E_{\text{LUMO}}$	[21, 22]
Electronegativity (χ)	$\chi = (IP + EA) / 2$	[22]
Hardness (η)	$\eta = (IP - EA) / 2$	[23]
Chemical potential (μ)	$\mu = -(IP - EA) / 2$	[24]
Electrophilicity index (ω)	$\omega = \mu^2 / 2\eta$	[22]
Maximum charge transfer (ΔN_{\max})	$\Delta N_{\max} = -\mu / \eta$	[45]

2.3.2. Nonlinear Optical Analysis

The total electric dipole moment (μ), linear polarizability (α), anisotropy of polarizability ($\Delta\alpha$) and first order hyperpolarizability (β) were investigated through DFT-based methods to reflect more reliable and accurate results.²⁵⁻²⁹ Threshold values of the unsubstituted thiophene derivatives and urea were calculated using DFT/B3LYP/ 6-311++G(d,p) as a level of theory. The optic parameters were obtained with the help of the following mathematical equations (Table 2).

The output files of Gaussian 09 W software provided the values of the mathematical portions and elements of the matrices. They were obtained as following: The total dipole moment components x, y, z had found under the heading “Dipole moment (field-independent basis, Debye):”, and (α_{xx} , α_{yy} and α_{zz}) for linear polarizability α and anisotropy of polarizability $\Delta\alpha$ values were estimated in electrostatic unit (esu) and found under heading “Quadrupole moment (field-independent basis, Debye-Ang):” Finally, the hyperpolarizability matrix elements (β_{xxx} , β_{xyy} , β_{xzz} , β_{yyy} , β_{yzz} , β_{yxx} , β_{zzz} , β_{zxx} and β_{zyy}) were found under title “Octapole moment (field-independent basis, Debye-Ang**2):”

Table 2. Non-linear optical parameters

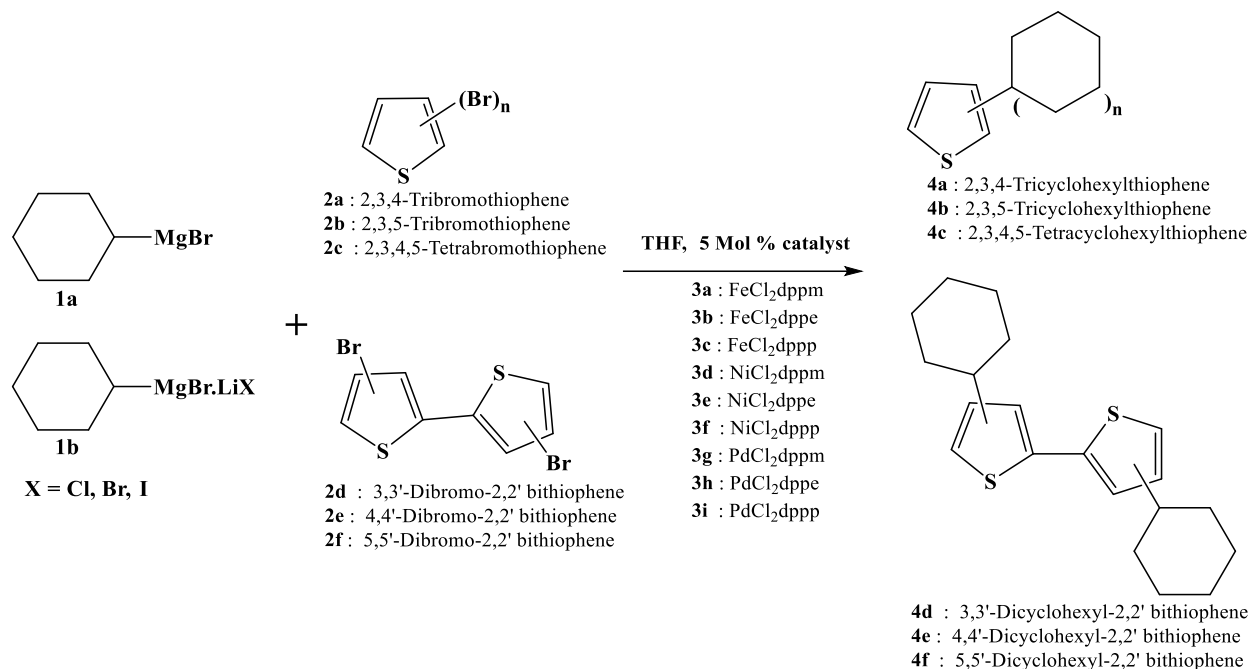
Non-linear optical parameter	equation	Reference
Total dipole moment (μ)	$\mu_{tot} = (\mu_x^2 + \mu_y^2 + \mu_z^2)^{\frac{1}{2}}$	[28]
Linear polarizability (α)	$(\alpha)_{tot} = \frac{1}{3}(\alpha_{xx} + \alpha_{yy} + \alpha_{zz})$	[28]
anisotropy of polarizability ($\Delta\alpha$)	$\Delta\alpha = \frac{1}{\sqrt{2}}[(\alpha_{xx} - \alpha_{yy})^2 + (\alpha_{yy} - \alpha_{zz})^2 + (\alpha_{zz} - \alpha_{xx})^2 + 6\alpha_{xz}^2 + 6\alpha_{xy}^2 + 6\alpha_{yz}^2]^{\frac{1}{2}}$	[28]
Hyperpolarizability (β)	$\beta = [(\beta_{xxx} + \beta_{xyy} + \beta_{xzz})^2 + (\beta_{yyy} + \beta_{yzz} + \beta_{yxx})^2 + (\beta_{zzz} + \beta_{zxx} + \beta_{zyy})^2]^{\frac{1}{2}}$	[28]

3. Results and Discussion

The coupling reaction protocol is illustrated in Scheme 1. The reaction of cyclohexylmagnesium bromide **1a** (1.2 equiv) with tribromothiophenes **2a-2b** (0.3 equiv), tetrabromothiophene **2c** (0.2 equiv) and symmetrical dibromo-2,2'-bithiophenes **2d-2f** (0.5 equiv), catalyzed by 5 mol% (PdCl₂dppa, NiCl₂dppa and FeCl₂dppa) **3a-3i**, at room temperature in THF, stirring for 24 h gave poor yields of the corresponding coupled products **4a-4f** (Table 3). Similarly, employing the widely used additives in coupling reactions, i.e. N, N, N',N'-tetramethylethylenediamine (10 mol%) (TMEDA) and trimethylamine (N(Et)₃), under vigorously stirred refluxing conditions generated poor yields (Table 2).¹⁶⁻¹⁹ Thus, the reaction seemed not dependent on high temperatures or nature the additives, although the yields were slightly improved by reflux.

Iron complexes as promising catalysts in cross coupling reactions have attracted a lot of attention owing to their economic and environment friendly reasons.^{18,19} Therefore, [FeCl₂(dppm)], [FeCl₂(dppe)] and [FeCl₂(dppp)] were synthesized to utilize them in the coupling reaction of cyclohexyl magnesium bromide with tri- and tetrabromothiophene and symmetrical dibromo-2,2'-bithiophene substrates under the same reaction conditions employed in palladium and nickel catalyzed cross-coupling reactions. [FeCl₂(dppm)] was found not an efficient catalyst in the reactions (Table 3), although its catalytic activity somewhat enhanced in the presence of TMEDA or N(Et)₃ (Table 4). In the light of seeking an efficient synthetic protocol for the coupling reactions, in the preliminary experiments, it was found that the addition of some lithium salts to cyclohexylmagnesium bromide as adducts enhanced the yields of the corresponding coupled products. Investigation of the effect of different lithium halide salts and their efficiency in the cross-coupling reaction showed that the coupling reaction was highly dependent on the choice of lithium halide adducts. Therefore, LiCl, LiBr and LiI salts were employed in the preparation of cyclohexylmagnesium bromide. Remarkably, the coupling reactions, conducted under the similar conditions, in the presence of LiCl salt, gave the cross-coupled products in good yields at the ambient temperature within one hour without employing any further additives (Table 5). Thus, after having the optimized conditions, the reaction was extended to the coupling of cyclohexyl moiety with tri-, tetrabromothiophene and symmetrical dibromo-2,2'-bithiophene substrates using various lithium halides salts as adducts with Grignard reagents **1b**. The reaction resulted in a dramatic increase in the yields of coupled products up to 95% yield (Table 6). Furthermore, the catalytic activity of FeCl₂dppm **3a** was extremely promoted with the coupling yields reaching to 80%. Surprisingly, PdCl₂dppp **3i** catalyst afforded excellent yields in term of the highest yield of cross-coupled products of **4b**, **4c** and **4e** in 98% yield within one hour at room temperature. In striking contrast, the coupling reactions in presence lithium iodide was found to be not effective (Table 7). Moreover, microwave-assisted cross-coupling of cyclohexylmagnesium bromide with tri-, tetrabromothiophene and symmetrical dibromo-2,2'-bithiophene substrates in the presence of only FeCl₂dppp **3c**, NiCl₂dppp **3f** and PdCl₂dppp **3i**, gave the cross-coupled products in relatively good yields at 50 °C within 20 minutes without employing any further additives (Table 8).

Optimization of Kumada cross-coupling reactions



Scheme 1. Cross-coupling reactions of cyclohexyl magnesium bromide or the corresponding LiCl, LiBr or LiI adducts with various tri-, tetra-bromothiophene and symmetrical di-bromo-2, 2' bithiophene derivatives employing different Fe, Ni and Pd precatalysts. a) 3 mol% **3a-i**, THF, room temperature and 24h.

Table 3. The yields of Kumada reaction of cyclohexyl magnesium bromide with tri-, tetra-bromothiophene and symmetrical di-bromo-2, 2' bithiophene derivatives using Pd, Ni and Fe catalysts, stirring at room temperature for 20 hours

Product	3a	3b	3c	3d	3e	3f	3g	3h	3i
4a	0	5	5	10	10	15	20	20	30
4b	5	10	10	10	10	20	10	10	20
4c	0	5	10	15	20	20	15	20	35
4d	5	5	15	10	20	25	10	20	40
4e	5	5	15	15	25	35	25	35	35
4f	0	10	20	10	25	30	10	15	25

Table 4. The yields of Kumada reaction of cyclohexylmagnesium bromide with tri-, tetra-bromothiophene and symmetrical di-bromo-2, 2' bithiophene derivatives using PdCl₂dppm, NiCl₂dppm and FeCl₂dppm catalysts: Effect of refluxing with TMEDA or N(Et)₃ for 20 hours.

Product	FeCl ₂ dppm (3a)			NiCl ₂ dppm (3d)			PdCl ₂ dppm (3g)		
	RF	TMEDA	N(Et) ₃	RF	TMEDA	N(Et) ₃	RF	TMEDA	N(Et) ₃
4a	12	15	10	25	15	25	30	40	35
4b	9	15	20	30	25	25	35	45	40
4c	10	20	15	20	25	35	30	30	35
4d	15	20	20	20	20	30	35	35	30
4e	10	15	25	20	10	15	35	20	35
4f	10	15	10	15	15	15	40	20	35

Table 5. The yields of Kumada reaction of cyclohexylmagnesium bromide lithium chloride adduct with tri-, tetra-bromothiophene and symmetrical di-bromo-2, 2' bithiophene derivatives using Pd, Ni and Fe catalysts, stirring at room temperature for 1 hour.

Product	3a	3b	3c	3d	3e	3f	3g	3h	3i
4a	45	50	55	45	55	55	55	65	70
4b	50	50	60	60	65	65	70	71	80
4c	44	47	55	50	50	60	60	72	83
4d	45	55	62	50	66	76	60	79	85
4e	50	65	65	58	71	80	70	75	85
4f	48	60	70	70	75	82	65	80	90

Table 6. The yields of Kumada reaction of cyclohexylmagnesium bromide lithium bromide adduct with tri-, tetra-bromothiophene and symmetrical di-bromo-2, 2' bithiophene derivatives using Pd, Ni and Fe catalysts, stirring at room temperature for 1 hour.

Product	3a	3b	3c	3d	3e	3f	3g	3h	3i
4a	60	65	75	63	75	90	77	90	95
4b	65	75	80	70	73	85	75	85	98
4c	63	65	75	65	75	90	80	85	98
4d	65	75	80	50	60	75	85	89	95
4e	50	65	75	70	80	85	65	85	98
4f	60	65	75	65	75	88	70	80	95

Table 7. The yields of Kumada reaction of cyclohexylmagnesium bromide lithium Iodide adduct with tri-, tetra-bromothiophene and symmetrical di-bromo-2, 2' bithiophene derivatives using Pd, Ni and Fe catalysts, stirring at room temperature for 1 hour.

Product	3a	3b	3c	3d	3e	3f	3g	3h	3i
4a	10	20	20	20	30	35	30	40	45
4b	20	30	35	25	35	45	25	30	30
4c	20	25	25	20	25	30	25	35	35
4d	10	15	25	15	25	35	20	30	40
4e	10	15	25	15	25	25	25	25	35
4f	15	25	30	15	30	40	20	25	35

Table 8. The yields of Microwave-assisted Kumada reaction of cyclohexyl magnesium bromide with tri-, tetra-bromothiophene and symmetrical di-bromo-2, 2' bithiophene derivatives using Pd, Ni and Fe catalysts, stirring at 50 °C for 20 min.

Product	3c	3f	3i
4a	40	40	60
4b	45	45	65
4c	55	50	60
4d	55	55	70
4e	45	55	60
4f	45	45	50

On the basis of these results, an efficient Grignard reagent with lithium salts (cyclohexylmagnesium bromide with LiX, X= Cl, Br and I), having an excellent solubility and stability in THF at room temperature, was generated, which led to considerable increase in yields in the presence of palladium, nickel and iron complexes as catalysts. The effect of lithium halides was attributed to the inhibition of the formation of polymeric aggregates of the Grignard compound during the preparation of the organometallic reagent, which might be responsible for acceleration of the homocoupling formation as a side product, resulting in a more reactive complex.^{34,35} Moreover, lithium halides played an important role in the enhancement of the

Optimization of Kumada cross-coupling reactions

nucleophilicity of Grignard reagent. The yields of the corresponding coupled products gradually increased in the order of $[MCl_2(dppp)] > [MCl_2(dppe)] > MCl_2(dppm)$ ($M = Pd, Ni, \text{ and } Fe$). This catalytic behavior was imputed to the influence of the bite angle of the ligands, which had an influential role in the reductive elimination stage. Catalytic cycles in cross coupling reactions contain three major steps; oxidative addition of C–X to the transition metal center, transmetalation to form active diorganometal transition state and finally a reductive elimination to generate the desired product and reform the catalytically active species. Reductive elimination is a crucial process including the interaction of two organic molecules together to construct a new C–C bond. However, expanding of the diphosphine bite angle leading to the compression of the angle Carbon-Metal-Carbon, forcing the two carbon atoms to be closer together, which will facilitate the formation of the bond between two carbon atoms.^{1,37}

3.1. DFT Modelling

3.1.1. Frontier Molecular Orbital's (FMO) and Reactivity Descriptors

The highest occupied molecular orbital (HOMO) and lowest unoccupied molecular orbital (LUMO) in gas phase and HOMO–LUMO energy gap (ΔE) were calculated for the coupled products (**4a–4f**) (Fig S13-S18). While the HOMO orbitals are relatively located over the structures of the coupled products,³⁸ the LUMO orbitals spreaded over the cyclohexyl substituents in compounds **4a**, **4b**, **4c** and **4f**, and concentrated at thiophene ring in **4d** and **4e**.

Some molecular properties like relative stability and non-linear optical (NLO) properties depend on the energy difference between HOMO and LUMO levels (ΔE).^{39–41} Energy gap (ΔE) between LUMO and HOMO is also play an influential role in determining the reactivity ranking, owing to the electron mobility. A molecule with small energy gap is more reactive and polarizable to be suitable candidate for useful NLO compounds.^{42,43} HOMO-LUMO energies were calculated in eV unit at gas phase, and in chloroform and acetone (Tables 9–11). In all cases, the energy gaps were found to be smaller than thiophene (gas phase 6.126, chloroform 6.130, acetone 6.133 eV), indicating that the cross-coupled products had non-linear optical response more than pure thiophene. In addition, these compounds provided a good environment for charge transfer in the chemical reactions. Chemical hardness (η) measures how a molecule resists the change of stability and electron distribution, hence, the chemical hardness is direct proportional to the chemical stability. The results in Table 9–11 demonstrate that thiophene and urea are harder than the coupled compounds **4a–4f** in the gas phase, and in chloroform and acetone. These results indicated an agreement with NLO properties, where soft molecule undergoes charge transfer process more easily.

Low electronegativities (Table 9-11) of the coupled compounds compared with urea and thiophene in all cases were consistent with the optical properties. Hence, the coupled molecules tend to have lower barriers for electronic charge entrance. In turn, the tendency to electronic escape from a stable molecular system known as chemical potential (μ),⁴⁵ where values of μ in the Tables below represent higher values than urea and thiophene, this physical entity reflects the changeable in the electronic cloud, which enhance the NLO properties.

Electrophilicity index (ω) was calculated to assign the stability of the system after accepting an electron. A molecule with high ω is considered as a good electrophile, while molecule with low ω will be a good nucleophile.⁴⁶ The calculations indicated an acceptable nucleophilic character of the coupled compounds, especially at thiophene ring site (Table 9). the Maximum charge transfer (ΔN_{\max}) is defined as a propensity of a molecular system to acquire an additional electronic charge.⁴⁶ The values in Tables 9-11. The compounds showed higher capacity toward charge transfer more than unsubstituted thiophene and urea (Tables 9-11), which directly assist in increasing of NLO properties of the compounds **4a–4f**.

Table 9. Molecular orbital energies and global chemical reactivity descriptors in gas phase in eV unit

Titled compound	E_{HOMO}	E_{LUMO}	E_{gap}	η	χ	μ	ω	ΔN_{max}
4a	-1.832	-0.804	1.028	0.514	1.318	-1.318	1.690	2.564
4b	-2.044	-0.948	1.097	0.548	1.496	-1.496	2.041	2.729
4c	-2.231	-0.898	1.333	0.666	1.565	-1.565	1.837	2.348
4d	-3.266	-0.761	2.505	1.252	2.013	-2.013	1.619	1.608
4e	-3.168	-0.718	2.449	1.225	1.943	-1.943	1.541	1.587
4f	-3.114	-0.821	2.293	1.147	1.968	-1.968	1.688	1.716
Thiophene	-6.675	-0.549	6.126	3.063	3.612	-3.612	2.129	1.179
Urea	-7.127	-1.414	5.713	2.856	4.270	-4.270	3.192	1.495

Table 10. Molecular orbital energies and global chemical reactivity descriptors in chloroform solvent in eV unit

Titled compound	E_{HOMO}	E_{LUMO}	E_{gap}	η	χ	μ	ω	ΔN_{max}
4a	-2.576	-0.810	1.766	0.883	1.693	-1.693	1.624	1.918
4b	-2.359	-0.820	1.540	0.770	1.590	-1.590	1.641	2.065
4c	-3.309	-0.996	2.313	1.156	2.152	-2.152	2.003	1.861
4d	-3.237	-0.913	2.324	1.162	2.075	-2.075	1.853	1.786
4e	-3.151	-1.082	2.069	1.034	2.116	-2.116	2.165	2.046
4f	-3.309	-0.996	2.313	1.156	2.152	-2.152	2.003	1.861
Thiophene	-6.711	-0.581	6.130	3.065	3.646	-3.646	2.169	1.190
Urea	-7.158	-1.440	5.719	2.859	4.299	-4.299	3.232	1.504

Table 11. Molecular orbital energies and global chemical reactivity descriptors in acetone solvent in eV unit

Titled compound	E_{HOMO}	E_{LUMO}	E_{gap}	η	χ	μ	ω	ΔN_{max}
4a	-2.828	-0.718	2.110	1.055	1.773	-1.773	1.490	1.681
4b	-2.625	-0.774	1.850	0.925	1.699	-1.699	1.561	1.837
4c	-2.432	-0.807	1.625	0.813	1.620	-1.620	1.614	1.993
4d	-3.337	-1.115	2.222	1.111	2.226	-2.226	2.229	2.003
4e	-3.280	-1.011	2.269	1.135	2.146	-2.146	2.029	1.891
4f	-3.177	-1.189	1.987	0.994	2.183	-2.183	2.398	2.197
Thiophene	-6.735	-0.602	6.133	3.066	3.669	-3.669	2.195	1.196
Urea	-7.177	-1.452	5.725	2.862	4.314	-4.314	3.251	1.507

3.1.2. Molecular electrostatic potential (MEP)

Physicochemical properties for the chemical compounds could be evaluated with electrostatic potential maps.⁴⁷ Polarity, electrophilic and nucleophilic sites of the molecule were visualized by means of

Optimization of Kumada cross-coupling reactions

electrostatic potential maps. In addition, charge density sites of the examined molecules were represented by different colors starting from red as the most negative charge to blue as the most positive charge.⁴⁸ Electronic densities in terms of molecular electrostatic potential (MEP) for the compounds **4a-4f** were calculated at the same level of theory of the energy calculations. Then, they were visualized using Gaussview 6.0 software, where the isodensity surfaces were mapped with ESP (electrostatic potential) under total density cube. The realistic transparent electrostatic potential maps for the titled compounds are presented in Figures S19–S24. The MEP maps of the coupled compounds **4a-4f** exhibited color spectrum from red to blue with same proximity electronic density distribution among the compounds. The most negative potential (electron rich) in the map appeared at thiophene ring, indicating a strong nucleophilicity and reactivity toward the electrophiles. While the carbon atoms of cyclohexyl groups, directly attached to the thiophene ring, exhibited an intermediate negative potential with yellow to orange color, the carbon and hydrogen atoms away from the thiophene ring showed zero to intermediate positive potential with green to cyan color, providing an electron deficient environment, which make them reactive toward nucleophiles.

3.1.3. Non-Linear Optical Properties (NLO)

Molecules having nonlinear optical properties (NLO) produce response to electromagnetic radiation.^{49,50} These compounds have a great importance in optoelectronic applications, such as the display devices, optical communication systems, optical switching, signal processing, optical computing and other significant applications.^{47,51} To determine NLO properties of organic compounds, some significant electronic and optical parameters, like total electrical dipole moment μ , main linear polarizability α , anisotropy of the polarizability $\Delta\alpha$ and first order hyperpolarizability β , which should be higher in than urea, need to be taken into account.⁵²

Herein, DFT calculations were implemented to evaluate the nonlinear optical properties (Table 12 and Figure S25). The coupled compounds **4a-4f** showed obviously higher values of linear polarizability α , anisotropy hyperpolarizability $\Delta\alpha$, and first order hyperpolarizability β compared to the standard urea (urea 0.359×10^{-23} , 5.666×10^{-24} and 0.177×10^{-31} in esu unit, respectively). Dipole moments of the coupled products were found to exhibit various values. The first order hyperpolarizability β values for compounds **4a, b, 4c** and **4f** were higher than those of urea and thiophene. Based on the DFT calculations, addition of cyclohexyl substituents to the thiophene ring led to enhancement of the NLO properties. For instance, the linear polarizability α increased by 2 and 4 folds compared to thiophene and urea, respectively. While the anisotropy of polarizability $\Delta\alpha$ increased in the presence of cyclohexyl substituents reaching 10 folds compared to thiophene and urea values, first order hyperpolarizability β of the coupled products (**4a-4c**) were in the range of 2 to 4 folds than urea. Accordingly, it could be concluded that thiophene containing compounds **4a-f4** are good candidates for NLO applications. Consequently, addition of cyclohexyl moiety to the thiophene ring remarkably modified the NLO parameters.

Table 12. Non-linear optical properties NLO of the titled compounds

Titled compound	μ (Debye)	α ($\times 10^{-23}$ esu)	$\Delta\alpha$ ($\times 10^{-24}$ esu)	β ($\times 10^{-31}$ esu)
4a	1.210	2.069	6.635	4.108
4b	3.593	2.145	5.400	2.300
4c	1.898	2.628	6.246	2.273
4d	0.057	1.892	10.37	0.190
4e	0.041	2.068	5.666	0.177
4f	0.061	1.948	8.991	0.203
Thiophene	0.380	0.533	1.122	0.034
Urea	3.007	0.359	1.071	1.451

4. Conclusion

Applying an optimized and straightforward Kumada-Corriu-Tamao cross-coupling protocol by using Tables, and available palladium, nickel, and iron together with diphenylphosphino alkane ligands to catalyze efficiently the couplings of cyclohexylmagnesium bromide with tri-, tetrabromothiophene and symmetrical dibromo-2,2'-bithiophenes are reported. The reaction requires only a relatively low loading of the catalyst (3 mol%) and completes within a short period of time (1 h). During the screening of lithium salts as an adduct with Grignard reagent, it was found that the nature of lithium salts was critical in achieving a high coupling yield. Lithium bromide gave superior results in the presence of Pd, Ni and Fe under the mild conditions. It significantly amended the catalytic activity of iron catalyst.-Moreover, DFT/B3LYP/6-311++G(d,p) approach was used to determine global chemical descriptors, FMOs, MEP maps and NLO properties for the coupled compounds **4a-4f**. The results showed that ΔE , chemical hardness, electronegativity and chemical potential are proportional with that of NLO properties.-Linear polarizability α , anisotropy hyperpolarizability $\Delta\alpha$ and first order hyperpolarizability β showed a higher values than urea at the same level of theory.

Acknowledgements

The authors gratefully thank Philadelphia University in Jordan for providing all the materials in the scientific laboratory to make this work possible.

Supporting Information

Supporting information accompanies this paper on <http://www.acgpubs.org/journal/organic-communications>

ORCID

Adnan A. Dahadha: [0000-0002-4160-0622](https://orcid.org/0000-0002-4160-0622)

Mohammad Abunuwar: [0000-0003-2639-4725](https://orcid.org/0000-0003-2639-4725)

Mohammad Al-Dhoun: [0000-0003-1768-0738](https://orcid.org/0000-0003-1768-0738)

Mohammad Hassan: [0000-0003-2531-9360](https://orcid.org/0000-0003-2531-9360)

Mohamed J. Saadh: [0000-0002-5701-4900](https://orcid.org/0000-0002-5701-4900)

References

- [1] Van Leeuwen, P. W. N. M.; Kamer, P. C. J.; Reek, J. N. H.; Dierkes, P. Ligand bite angle effects in metal-catalyzed C–C bond formation. *Chem. Rev.* **2000**, *100*, 2741–2770.
- [2] Dahadha, A. A.; Aldhoun, M. M.; Hassan, M.; Ibrahim, Q. A.; Talat, N. T. Carbon-carbon cross-coupling reactions of organomagnesium reagents with a variety of electrophilic substrates mediated by iron catalysts. *Org. Commun.* **2021**, *14* (1), 1-38.
- [3] Bolm, C.; Legros, J.; Le Paih, J.; Zani, L. Iron-catalyzed reactions in organic synthesis. *Chem. Rev.* **2004**, *104* (12), 6217–6254.
- [4] Dahadha, A. A. Cobalt, copper, and chromium catalyzed carbon-carbon coupling reactions using a broad spectrum of Grignard reagents as reaction partners. *Arkivoc* **2019**, *1*, 106-138.
- [5] Czaplik, W. M.; Mayer, M.; Cvengroš, J.; Wangelin, A. J. Coming of age: sustainable iron-catalyzed cross-coupling reactions. *ChemSusChem.* **2009**, *2* (5), 396–417
- [6] Korch, K. M.; & Watson, D. A. (2019). Cross-coupling of heteroatomic electrophiles. *Chem. Rev.* **2019**, *119* (13), 8192-8228.
- [7] Dahadha, A.; Aldhoun, M. Nickel and palladium catalyzed Kumada-Tamao-Corriu cross-coupling reactions: scope and recent advances. *Arkivoc* **2018**, *vi*, 234-253.

Optimization of Kumada cross-coupling reactions

- [8] Negishi, E. Palladium- or nickel-catalyzed cross coupling. A new selective method for carbon-carbon bond formation. *Acc. Chem. Res.* **1982**, *15* (11), 340-348.
- [9] Hooshmand, S. E.; bahreh, H.; Sedghi, R.; Varma, R. S. Recent advances in the Suzuki-Miyaura cross-coupling reaction using efficient catalysts in eco-friendly media. *Green Chem.* **2018**. doi:10.1039/c8gc02860e
- [10] Nikoofard, H.; Gholami, M. (2014). Theoretical investigation of structures and electronic states of a series of phenyl-capped oligothiophenes. *C R Chimie.* **2014**, *17* (10), 1034–1040.
- [11] Masui, K.; Ikegami, H.; & Mori, A. Palladium-Catalyzed C–H Homocoupling of thiophenes: facile construction of bithiophene structure. *J. Am. Chem. Soc.* **2004**, *126* (16), 5074–5075.
- [12] Le, T.-H.; Kim, Y.; Yoon, H. Electrical and electrochemical properties of conducting polymers. *Polymers* **2017**, *9* (12), 150, doi:10.3390/polym9040150 10.3390/polym9040150.
- [13] Dekker, M.; Skotheim, T.; Reynolds, J.; Elsembamer, R. *Handbook of Conducting Polymers*. 2nd Edition, Inc. New York, NY, USA, 1998.
- [14] Locklin, J.; Li, D.; Mannsfeld, S. C. B.; Borkent, E.-J.; Meng, H.; Advincula, R.; Bao, Z. Organic thin film transistors based on cyclohexyl-substituted organic semiconductors. *Chem. Mater.* **2005**, *17* (13), 3366–3374.
- [15] Yoshino, K.; Takahashi, H.; Muro, K.; Ohmori, Y.; Sugimoto, R. Optically controlled characteristics of Schottky gated poly(3-alkylthiophene) field effect transistor. *J. Appl. Phys.* **1991**, *70* (9), 5035–5039.
- [16] Vechorkin, O.; Proust, V.; Hu, X. functional group tolerant Kumada–Corriu–Tamao coupling of nonactivated alkyl halides with aryl and heteroaryl nucleophiles: catalysis by a nickel pincer complex permits the coupling of functionalized Grignard reagents. *J. Am. Chem. Soc.* **2009**, *131* (28), 9756–9766.
- [17] Dahadha, A. A.; Imhof, W. A comprehensive study of the effects of spectator ligands, transition metals and lithium halide additives on the efficiency of iron, nickel and palladium-catalyzed cross-coupling reactions of cyclohexyl magnesium bromide with fluorinated bromobenzene. *Arkivoc* **2013**, (iv), 200-216.
- [18] Czaplik, W. M.; Mayer, M.; Jacobi von Wangelin, A. Domino iron catalysis: direct aryl-alkyl cross-coupling. *Angew. Chem. Int. Ed.* **2009**, *48* (3), 607–610.
- [19] Bedford, R. B.; Brenner, P. B.; Carter, E.; Cogswell, P. M.; Haddow, M. F.; Harvey, J. N.; Woodall, C. H. (2014). TMEDA in iron-catalyzed Kumada Coupling: amine adduct versus homoleptic “ate” complex formation. *Angew. Chem. Int. Ed.* **2014**, *53* (7), 1804–1808.
- [20] Zhang, B.; Han, G.; Wang, Y.; Chen, X.; Yang, Z.; Pan, S. Expanding frontiers of ultraviolet nonlinear optical materials with fluorophosphates. *Chem. Mater.* **2018**, *30* (15), 5397-5403.
- [21] Jawaria, R.; Hussain, M.; Khalid, M.; Khan, M. U.; Tahir, M. N.; Naseer, M. M.; Shafiq, Z. Synthesis, crystal structure analysis, spectral characterization and nonlinear optical exploration of potent thiosemicarbazones based compounds: A DFT refine experimental study. *Inorganica Chim. Acta.* **2019**, *486*, 162-171.
- [22] Beytur, M.; Avinca, I. Molecular, electronic, nonlinear optical and spectroscopic analysis of heterocyclic 3-substituted-4-(3-methyl-2-thienylmethyleneamino)-4, 5-dihydro-1H-1, 2, 4-triazol-5-ones: experiment and DFT calculations. *Heterocycl Comm.* **2021**, *27* (1), 1-16.
- [23] Shehzad, F. K.; Khan, Q. U.; Mahmood, Q.; Ghafoor, F.; Alsaab, H. O.; Shah, S. A. A.; Iqbal, A. Third order NLO and second hyperpolarizability of functional porphyrin based polyimides. *Opt. Mater.* **2022**, *127*. doi:10.1016/j.optmat.2022.112317
- [24] Xu, J.; Li, X.; Xiong, J.; Yuan, C.; Semin, S.; Rasing, T.; Bu, X. H. Halide perovskites for nonlinear optics. *Adv. Mater.* **2020**, *32* (3), e1806736, doi:10.1002/adma.201806736.
- [25] Adant, C; Dupuis, M; Bredas, J. L. Ab initio study of the nonlinear optical properties of urea: electron correlation and dispersion effects. *Quantum chem. symp.* **1995**. *56*(Supplement 29), 497–507.
- [26] Çakmak, O.; Ersanlı, C. C.; Akar, K. B.; Karaoğlan, N. Structural, spectroscopic, Hirshfeld surface and DFT approach of 3,9-dibromophenanthrene. *Org. Commun.* **2022**, *15* (1), 59–70.
- [27] Baroudi, B.; Argoub, K.; Hadji, D.; Benkouider, A. M.; Toubal, K.; Yahiaoui, A.; Djafri, A. Synthesis and DFT calculations of linear and nonlinear optical responses of novel 2-thioxo-3-N, (4-methylphenyl) thiazolidine-4 one. *J. Sulfur Chem.* **2020**, *41* (3), 310–325.
- [28] Huang, Y.; Fan, X.; Chen, S. C. Zhao, N. Emerging technologies of flexible pressure sensors: materials, modeling, devices, and manufacturing. *Adv. Funct. Mater.* **2019**, *29* (12), doi:10.1002/adfm.201808509.
- [29] Barclay, J. E.; Leigh, G. J.; Houlton, A.; Silver, J. Mössbauer and preparative studies of some iron(II) complexes of diphosphines. *J. Chem. Soc., Dalton Trans.* **1988**, *11*, 2865–2870.

- [30] Noskowska, M.; Śliwińska, E.; Duczmal, W. Simple fast preparation of neutral palladium(II) complexes with SnCl₃ and Cl ligands. *Transit. Met. Chem.* **2003**, *28* (7), 756–759.
- [31] Steffen, W. L.; Palenik, G. J. Crystal and molecular structures of dichloro[bis(diphenylphosphino)methane]palladium(II), dichloro[bis(diphenylphosphino)ethane]palladium(II), and dichloro[1,3-bis(diphenylphosphino)propane]palladium(II). *Inorg. Chem.* **1976**, *15* (10), 2432–2439.
- [32] Watson, S. C.; Eastham, J. F. Colored indicators for simple direct titration of magnesium and lithium reagents. *J. Organomet. Chem.* **1967**, *9* (1), 165–168.
- [33] Perrin, D.D.; Armarego, W.L.F.; Perrin, D.R. *Purification of Laboratory Chemicals*, Pergamon Press, New York, 1980.
- [34] Scott, W. J.; Stille, J. K. Palladium-catalyzed coupling of vinyl triflates with organostannanes. Synthetic and mechanistic studies. *J. Am. Chem. Soc.* **1986**, *108* (11), 3033–3040.
- [35] Krasovskiy, A.; Knochel, P. A LiCl-Mediated Br/Mg exchange reaction for the preparation of functionalized aryl- and heteroaryl magnesium compounds from organic bromides. *Angew. Chem. Int. Ed.* **2004**, *43* (25), 3333–3336.
- [36] Krasovskiy, A.; Krasovskaya, V.; Knochel, P. Mixed Mg/Li amides of the type R₂NMgCl·LiCl as Highly efficient bases for the regioselective generation of functionalized aryl and heteroaryl magnesium compounds. *Angew. Chem. Int. Ed.* **2006**, *45* (18), 2958–2961.
- [37] Birkholz (née Gensow), M.-N.; Freixa, Z.; van Leeuwen, P. W. N. M. Bite angle effects of diphosphines in C–C and C–X bond forming cross coupling reactions. *Chem. Soc. Rev.* **2009**, *38* (4), 1099–1118.
- [38] Chaudhary, A.; Rath, S. P. Encapsulation of tenq and the acridinium ion within a bisporphyrin cavity: synthesis, structure, and photophysical and HOMO–LUMO-gap-mediated electron-transfer properties. *Chem. Eur. J.* **2012**, *18* (24), 7404–7417.
- [39] Aihara, J. I. Reduced HOMO–LUMO gap as an index of kinetic stability for polycyclic aromatic hydrocarbons. *J. Phys. Chem. A.* **1999**, *103* (37), 7487–7495.
- [40] Chemla, D. S. (Ed.). *Nonlinear Optical Properties of Organic Molecules and Crystals* (Vol. 1). Elsevier, 2012
- [41] Khoo, I. C.; Wu, S. T. *Optics and nonlinear optics of liquid crystals* (Vol. 1). World Scientific, 1993
- [42] Manolopoulos, D. E.; May, J. C.; Down, S. E. Theoretical studies of the fullerenes: *Chem. Phys. Lett.* **1991**, *18* (2-3), 105–111.
- [43] Sosa, C.; Andzelm, J.; Elkin, B. C.; Wimmer, E.; Dobbs, K. D.; Dixon, D. A. A local density functional study of the structure and vibrational frequencies of molecular transition-metal compounds. *J. Phys. Chem.* **1992**, *96* (16), 6630–6636.
- [44] Parthasarathi, R.; Padmanabhan, J.; Subramanian, V.; Sarkar, U.; Maiti, B.; Chattaraj, P. Toxicity analysis of benzidine through chemical reactivity and selectivity profiles: a DFT approach. *Internet Electron. J. Mol. Des.* **2003**, *2* (12), 798–813.
- [45] Babu, N. S.; Jayaprakash, D. Global and reactivity descriptors studies of cyanuric acid tautomers in different solvents by using of density functional theory (DFT). *Int. J. Sci. Res.* **2015**, *4* (6), 615–620.
- [46] Turkoglu G. Triarylborane functionalized selenophenothiophene analogues: Syntheses, photophysical and electrochemical properties. *Org. Commun.* **2018**, *11* (1), 12–22.
- [47] Ramachandran, G.; Muthu, S.; Uma Maheswari, J. (2013). Density functional theory and Ab initio studies of vibrational spectroscopic (FT-IR, FT-Raman and UV) first order hyperpolarizabilities, NBO, HOMO–LUMO and TD-DFT analysis of the 1,2-Dihydropyrazolo (4,3-E) Pyrimidin-4-one. *Solid State Sci.* **2013**, *16*, 45–52.
- [48] Balachandran, V.; Murugan, M.; Karpagam, V.; Karnan, M.; Ilango, G. Conformational stability, spectroscopic (FT-IR & FT-Raman), HOMO–LUMO, NBO and thermodynamic function of 4-(trifloromethoxy) phenol. *Spectrochim. Acta A Mol. Biomol.* **2014**, *130*, 367–375.
- [49] Nalwa, H.S., Miyata, S. (eds.): *Nonlinear Optics of Organic Molecules and Polymers*. CRC Press, New York, 1997
- [50] Prasad, P.N.; Williams, D.J. *Introduction to Nonlinear Optical Effects in Molecules and Polymers*. Wiley, New York, 1991

Optimization of Kumada cross-coupling reactions

- [51] Arjunan, V.; Mohan, S. Fourier transform infrared and FT-Raman spectra, assignment, ab initio, DFT and normal co-ordinate analysis of 2-chloro-4-methylaniline and 2-chloro-6-methylaniline. *Spectrochim. Acta A Mol. Biomol.* **2009**, *72* (2), 436–444.
- [52] Abdou, A.; Omran, O. A.; Nafady, A.; Antipin, I. S. Structural, spectroscopic, FMOs, and non-linear optical properties exploration of three thiaicax (4) arenes derivatives. *Arab. J. Chem.* **2022**, *15* (3), 103656, doi:10.1016/j.arabjc.2021.103656.

A C G
publications

© 2022 ACG Publications